metals

MDPI

Article

Prediction of Creep Rupture Life of 5Cr-0.5Mo Steel Using Machine Learning Models

Muhammad Ishtiaq [1], Hafiz Muhammad Rehan Tariq [2], Devarapalli Yuva Charan Reddy [3], Sung-Gyu Kang [1,*] and N.S. Reddy [4,*]

[1] New Materials Engineering, Gyeongsang National University, Jinju, 52828, South Korea; ishtiaq145@gnu.ac.kr
[2] Department of Mechanical Engineering, Incheon National University, Incheon 22012, Republic of Korea; 202221057@inu.ac.kr
[3] Chaitanya Bharathi Institute of Technology, Department of Artificial Intelligence and Machine Learning (AI&ML), Gandipet, Hyderabad, Telangana, India
[4] New Materials Engineering, Engineering Research Institute, Gyeongsang National University, Jinju, 52828, South Korea
* Correspondence: S.G. Kang; s.kang@gnu.ac.kr ,N.S. Reddy: nsreddy@gnu.ac.kr

Abstract: The creep rupture life of 5Cr-0.5Mo steels used in high-temperature applications is significantly influenced by factors such as minor alloying elements, hardness, austenite grain size, non-metallic inclusions, service temperature, and applied stress. The relationship of these variables with the creep rupture life is quite complex. In this study, the creep rupture life of 5Cr-0.5Mo steel was predicted using various machine learning (ML) models. To achieve higher accuracy, various ML techniques including random forest (RF), gradient boosting (GB), linear regression (LR), artificial neural network (ANN), ada boost (AB), and extreme gradient boosting (XGB) were applied with careful optimization of hidden parameters. Among these, the ANN-based model demonstrated superior performance, yielding high accuracy with minimal prediction errors for the test dataset (RMSE= 0.069, MAE=0.053, MAPE= 0.014, and R^2= 1). Additionally, we developed a user-friendly graphical user interface (GUI) for the ANN model, enabling users to predict and optimize creep rupture life. This tool helps materials scientists and industrialists prevent failures in high-temperature applications and design steel compositions with enhanced creep resistance.

Keywords: 5Cr-0.5Mo steel; Creep rupture life; Machine learning; Composition; Temperature; Stress

Academic Editor(s): Name

Received: date
Revised: date
Accepted: date
Published: date

Citation: Ishtiaq, M.; Tariq, H.M.R.; Reddy, D.Y.C.; Kang, S.-G.; Reddy, N.S. Prediction of Creep Rupture Life of 5Cr-0.5Mo Steel Using Machine Learning Models. *Metals* **2025**, *15*, x. https://doi.org/10.3390/xxxxx

1. Introduction

The ever-growing global population continues to drive an increasing demand for energy to support technological advancements and industrial operations. This has led to a critical need for high-performance industrial components capable of extending machinery life and minimizing operational shutdowns. To achieve maximum operational efficiency, it is essential to assess the lifespan of components in industrial equipment, particularly those operating under high-temperature conditions. Power plants and petrochemical industries widely use Cr-Mo steels due to their excellent high-temperature performance [1]. Among these, 5Cr-0.5Mo steel is one of the most important alloys in the Cr-Mo steel family, extensively utilized in manufacturing high-temperature components for

power generation devices [2]. The composition of the steel, particularly the addition of minor alloying elements, significantly affects its properties and performance [3, 4]. Additionally, initial cooling conditions—such as cooling temperature and cooling rates—play a vital role in determining the resultant austenite grain size and hardness, which are critical factors influencing the steel's mechanical behavior and service life [5]. Furthermore, the surrounding environment in particular applied stress during service is another decisive factor affecting the remaining life of components [6, 7]. However, the interplay of these variables is complex and non-linear, making it challenging to establish a clear understanding through conventional experimental approaches. During prolonged exposure to elevated temperatures and sustained stress, materials undergo specific changes that can significantly affect their properties [8], particularly the remaining service life. The application of stress can result in localized stress concentrations [9], the development of dislocation networks [10], and phase transformations [11, 12]. Additionally, exposure to high temperatures can alter phase fractions [11], promote the formation of secondary precipitates/carbides [13, 14], and ultimately lead to a reduction in creep resistance [15]. While numerous experimental studies have investigated the effects of these factors on the microstructure and performance of Cr-Mo steels [11, 16-20], a comprehensive analysis over broader intervals is lacking. Conducting such detailed experiments would require significant energy, resources, and time. Consequently, there is a pressing need for predictive modeling approaches that leverage existing data to forecast material behavior effectively. Some indirect methods have also been employed to estimate the creep rupture life, such as by analyzing the growth of oxide scales [21].

Researchers have utilized various machine learning (ML) models to predict various properties of metallic materials [22-25]. For example, Zhang et al. [26] predicted the creep rupture life of 316L stainless steel using linear regression (LR), random forest (RF), and artificial neural network (ANN) models. Similarly, Tan et al. [27] applied multiple models to predict the creep rupture life of 9Cr martensitic steels and compared their prediction accuracies. Xiang et al. [28] employed a deep-learning model to predict the creep rupture life of Fe-Cr-Ni alloys. The creep rupture life of low alloy steel was predicted by Wang et al. [29] by combining the ML model with genetic algorithms.

Although various ML methods have been applied to predict the properties of different materials, to the best of our knowledge, no significant research has been published on predicting the creep rupture life of 5Cr-0.5Mo steel using ML techniques, particularly artificial neural networks (ANN). This study aims to predict the creep rupture life of 5Cr-0.5Mo steel using multiple ML models and compare their accuracies using evaluation metrics such as root mean square error (RMSE), mean average error (MA E), mean average percentage error (MAPE), and R-squared (R^2). The most accurate model will be identified and recommended. In addition to predicting creep rupture life, the model will assess the influence of each input variable on the output. Furthermore, a user-friendly graphical user interface (GUI) will be developed to facilitate practical applications.

The proposed model is expected to provide significant benefits to the steel industry and materials engineers involved in the production of 5Cr-0.5Mo steels for high-temperature applications. Additionally, it will assist engineers working on the safety and reliability of power plant components.

2. Materials and Methods

2.1. Data Collection

The data required for the development of the model, including its training and testing phases, was obtained from the existing dataset provided by the National Institute for Materials Science (NIMS). This dataset includes critical parameters such as the chemical

composition, austenite grain size, non-metallic inclusion content, applied stress, service temperature, and the resulting creep rupture life of 5Cr-0.5Mo steel. A total of 237 datasets were obtained out of which 191 were used for training the model and the remaining 46 were used for testing the developed model. The statistical analysis of the data used for model training and testing is provided in Table 1.

Table 1. Summary of the statistical data of 5Cr-0.5Mo steel for model training and testing.

Variable	Training Data				Testing Data			
	Max	**Min.**	**Mean**	**Std. Dev.**	**Max.**	**Min.**	**Mean**	**Std. Dev.**
C	0.12	0.09	0.108	0.01	0.12	0.09	0.108	0.012
Si	0.37	0.27	0.331	0.012	0.37	0.27	0.33	0.035
Mn	0.56	0.44	0.499	0.035	0.56	0.44	0.499	0.048
P	0.022	0.007	0.016	0.048	0.022	0.007	0.015	0.005
S	0.01	0.005	0.007	0.005	0.012	0.005	0.007	0.002
Ni	0.083	0.043	0.060	0.003	0.083	0.043	0.060	0.015
Cr	5.02	4.61	4.84	0.016	5.02	4.61	4.84	0.150
Mo	0.52	0.49	0.503	0.151	0.52	0.49	0.504	0.010
Cu	0.13	0.05	0.072	0.031	0.13	0.05	0.073	0.030
Al	0.008	0.004	0.006	0.001	0.008	0.004	0.006	0.001
N	0.018	0.01	0.014	0.002	0.178	0.010	0.014	0.003
AGS	6.9	4.8	5.97	0.587	6.9	4.8	5.97	0.580
HBR	90	75	81	5.620	90	75	81	5.588
NMI	0.2	0.03	0.086	0.045	0.2	0.03	0.086	0.044
Temp.	650	500	562	52.90	650	500	562	52.90
Stress	216	29	89	50	265	29	95	58
Creep Life	5.12	1.37	3.64	0.99	5.06	1.58	3.62	1.00

2.2. Correlation Analysis

Pearson's correlation coefficient was utilized to evaluate the relationship between input and output variables. The coefficient values range from -1 to +1, and these are visually represented in a heatmap as shown in Figure 1. For better visualization, the color intensity corresponds to the magnitude of the linear relationships between the variables. A higher color intensity indicates a stronger relationship, with the strongest relationships, such as a variable's correlation with itself, represented in red and having the maximum value of +1. Furthermore, relatively strong positive relationships, such as that of carbon (C) with phosphorus (P), aluminum (Al), nitrogen (N), austenite grain size, and hardness (HRB), are depicted in shades of red. However, the intensity is slightly lower as these coefficients are positive but less than +1, typically exceeding 0.5. Conversely, the negative correlation of C with temperature is evident, aligning with the known phenomenon that higher temperatures adversely affect the strength imparted by carbon in steels. To aid in precise interpretation, the actual correlation coefficient values are displayed within each heatmap cell, providing a clearer understanding of the dependency between variables.

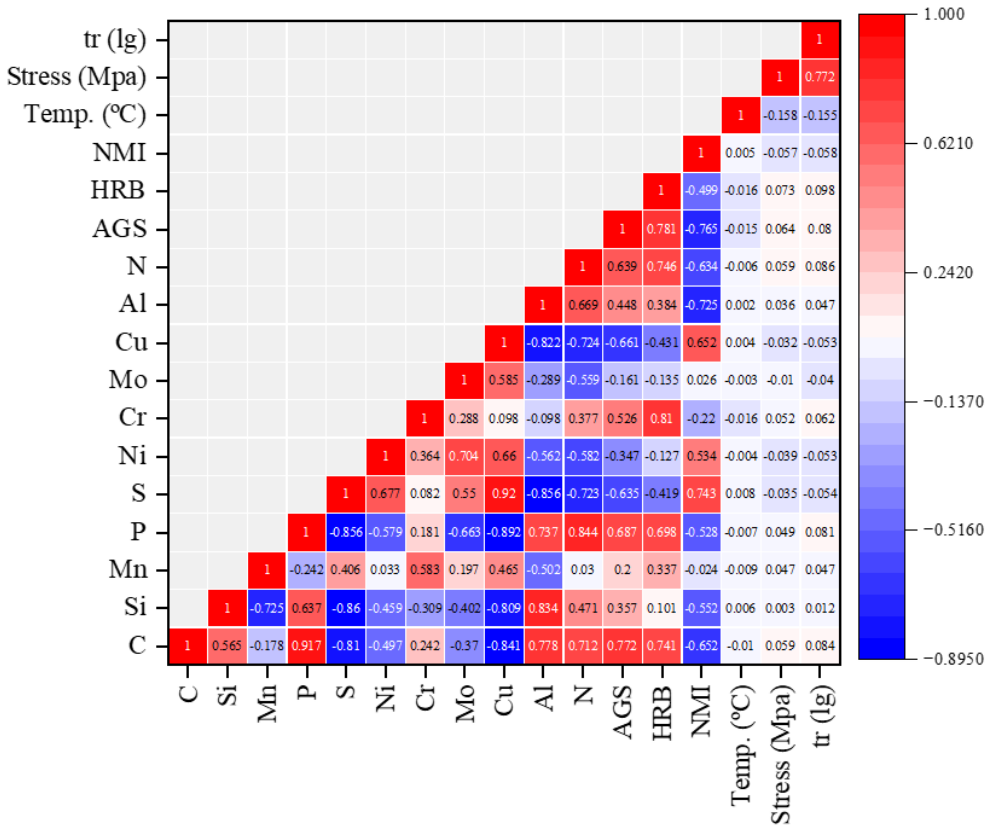

Figure 1. Heatmap illustrating the Pearson's correlation coefficient for the variables analyzed in this study. Each square contains the corresponding coefficient value, while the color intensity represents the strength of the relationship: darker shades indicate stronger correlations and lighter shades signify weaker relationships.

2.3. Data Preprocessing

The normalization function was employed to scale all the data within the range of 0.1 to 0.9. This approach improved the stability and performance of the model by preventing the generation of complex or extreme values. The normalization process was carried out using Equation 1.

$$Xn = \left(\frac{(X - X\,min) * 0.8}{(Xmax - Xmin)}\right) + 0.1 \quad (1)$$

Here X_n represents the normalized value, X_{max} is the maximum value, and X_{min} is the minimum value.

Once the optimal model was established, the normalized data were reverted to their original scale using Equation 2.

$$X = \left(\frac{(Xn - 0.1) * (Xmax - X\,min)}{8}\right) + Xmin \quad (2)$$

2.3. ML Methods

We applied six different machine learning methods to predict the creep rupture life of 5Cr-0.5Mo steel. These methods include (i) RF, (ii) GB, (iii) LR, (iv) ANN, (v) AB, and (vi) XGB.

These ML methods were first trained using a training dataset and then tested using a testing dataset. A schematic representation of the workflow for predicting the creep life of 5Cr-0.5Mo steels is illustrated in Figure 2.

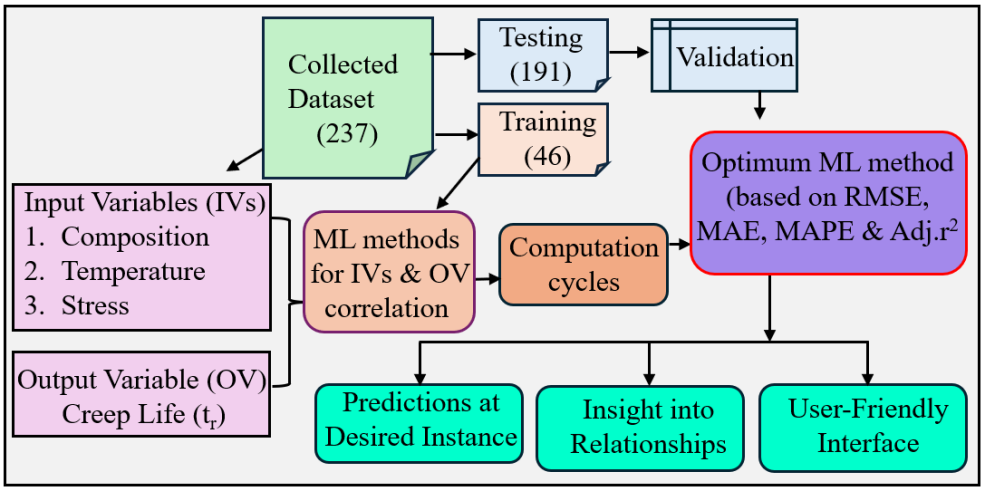

Figure 2. Schematic representation showing the steps involved in the present work.

2.4. Performance Evaluation

To evaluate the performance of each, metrics such as RMSE, MAE, MAPE, and R^2 values were calculated. The calculation formulas for RMSE, adj. R^2, MAE, and MAPE are presented in Equations 3, 4,5, and 6 respectively.

$$RMSE = \sqrt{\frac{1}{N}\sum_{i=1}^{N}(E_i - E_p)^2} \quad (3)$$

$$Adjusted\ R^2 = 1 - \frac{(1-R^2)(N-1)}{N-p-1}$$

$$MAE = \frac{1}{N}\sum_{i=1}^{N}\left|E_i - E_p\right| \quad (5)$$

$$MAPE = \frac{1}{N}\sum_{i=1}^{N}\left|\frac{E_i - E_p}{E_i}\right| \quad (6)$$

Here, N = number of data, Ei = actual values, Ep = predicted values, p = number of independent variables I = variable i.

The model configurations were optimized by minimizing these error metrics. Various configurations were tested. The configuration yielding the minimum error was identified as the optimal setup.

4. Results and Discussion

4.1. ML methods and their predictability

We optimized hyperparameters such as the learning rate, momentum term, number of hidden layers, and neurons for different models, selecting the parameters that yielded the lowest prediction errors. The performance of each model was then evaluated using RMSE, MAE, MAPE, and R^2, with the results presented graphically.

Figure 3(a) illustrates the RMSE, MAE, and MAPE values for the training dataset, while Figure 3(b) presents the corresponding values for the testing dataset. Since R^2 can reach a maximum value of 1, it is displayed separately in Figure 3(c) for both the training and testing datasets across all models.

For the testing dataset, the ANN model demonstrated the highest accuracy, achieving RMSE = 0.069, MAE = 0.053, MAPE = 0.014, and R^2=1. These results highlight the exceptional capability of the ANN model in predicting the creep rupture life of 5Cr-0.5Mo steel with the highest accuracy.

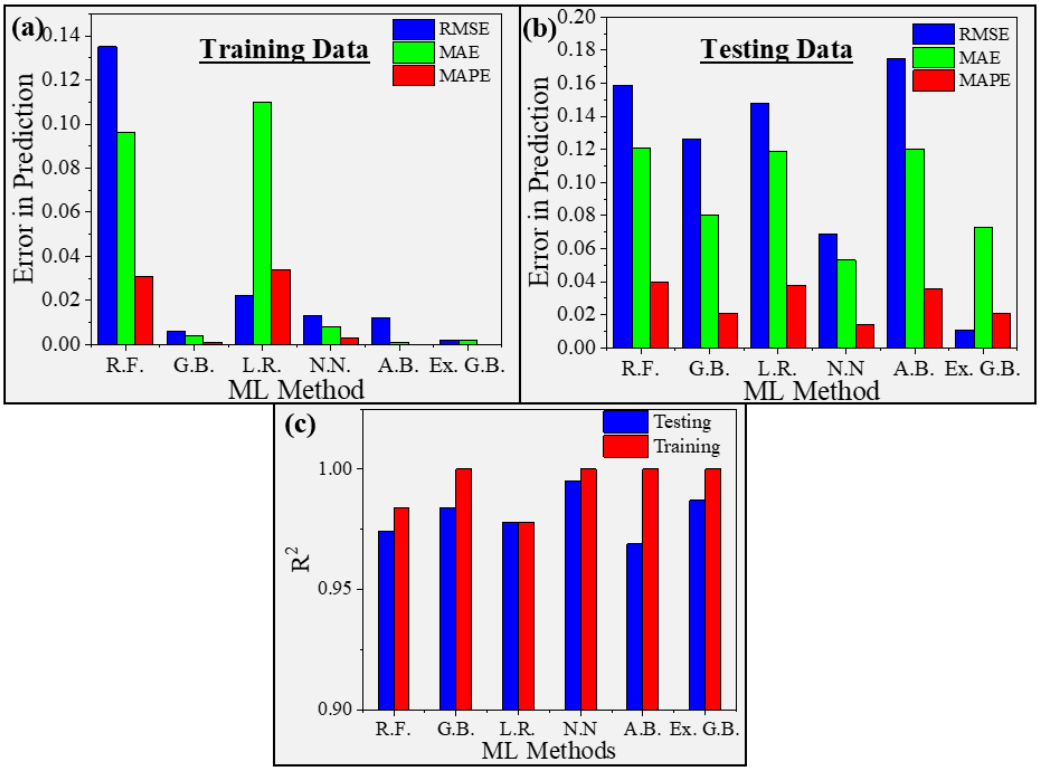

Figure 3. Graphical representation of the performance evaluation of various machine learning methods, (a) for training data (b) for testing data. (c) R2 for testing and training data. The smaller values of RMSE, MAE, and MAPE represent higher accuracy. The higher values~1 for R^2 represent better predictability.

Given the superior performance of the ANN model, it was utilized to predict the influence of various input parameters on the creep rupture life of 5Cr-0.5Mo steel. We will now provide a detailed discussion of the results obtained from the ANN model.

4.2. Prediction of the effect of input variables on Creep Rupture life

The ANN-based GUI generates a large volume of results through sensitivity analysis by systematically varying input parameters and assessing their impact on the output. However, due to the vast number of possible variations, it is impractical to represent all results comprehensively. To maintain clarity and relevance, we selectively present only two key sensitivity analyses that provide the most insightful or significant findings related to the study objectives. This ensures that the results remain interpretable and aligned with the research focus.

The dataset used for training and testing the model consisted of a limited number of entries. Despite this, the model was effectively trained to predict the creep rupture life of 5Cr-0.5Mo steel with high accuracy. For example, the dataset included only a few values for applied stress and corresponding time-to-rupture data. Specifically, for 650 °C, stress values were limited to 29, 37, 47, and 61 MPa, while for 500°C, higher stress values such as 137, 157, 177, and 216 MPa were available. The developed model, however, was capable of making predictions for nearly 100 different stress values ranging from 29 MPa to approximately 275 MPa across all temperatures (500 °C, 550 °C, 600 °C, and 650 °C), even in the absence of experimental data for some of these combinations.

Figure 4 provides a comparison between the experimental and predicted results, illustrating the effect of stress on time-to-rupture values at these temperatures. Figure 4 (a) demonstrates that the experimental data closely align with the predictions of the ANN model, with points lying on the same trend line. Figures 4 (b-d) depict the relationship

between stress and time-to-rupture at constant temperatures of 550 °C, 600 °C, and 650 °C, respectively. From a metallurgical perspective, at a constant temperature, the applied stress inversely affects the creep rupture life of 5Cr-0.5Mo steel. The magnitude of the applied stress significantly influences the microstructural changes occurring at that particular temperature. In some cases, stress can induce phase transformations, such as the transformation from austenite to martensite, a phenomenon known as transformation-induced plasticity (TRIP). Higher applied stress facilitates greater dislocation movement, thereby promoting early deformation and reducing the creep rupture life. Interestingly, the model effectively captured the trends in time-to-rupture as a function of stress, even without being explicitly provided with metallurgical principles underlying these variations. This capability underscores the robustness of the developed ANN model.

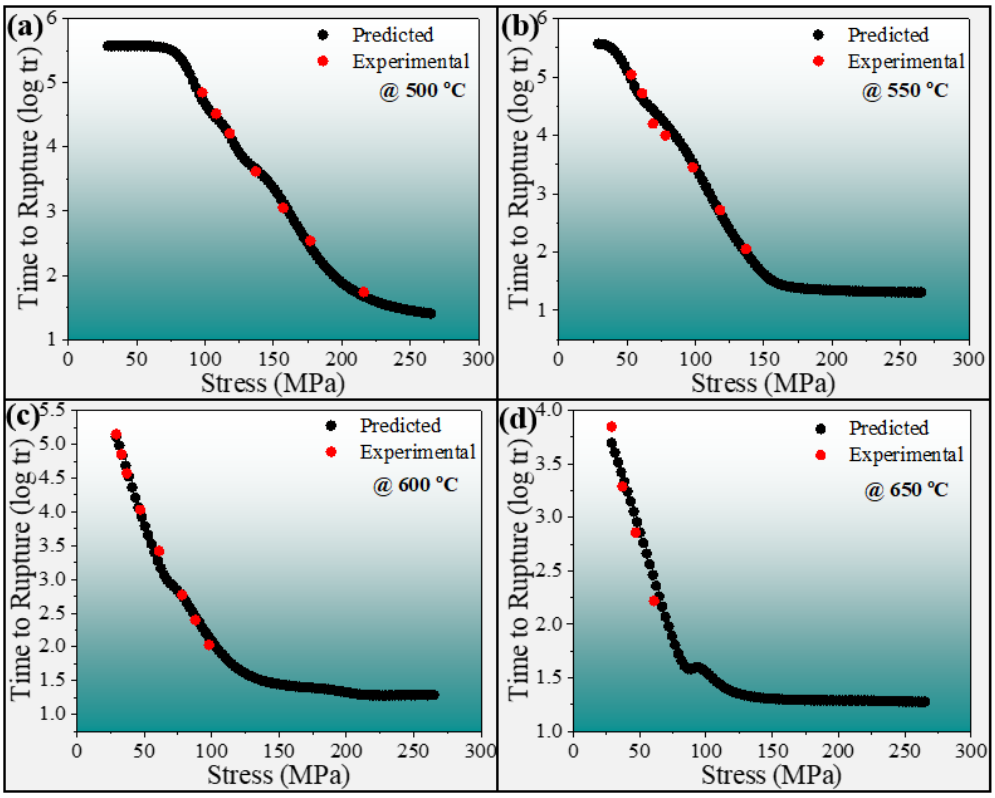

Figure 4. Graphical representation of the effect of applied stress on the creep rupture life of 5Cr-0.5Mo steel. The red color is for experimental and the black color is for prediction from ANN model.

As the temperature increases, dislocation motion becomes easier, leading to a reduction in the material's strength. This effect of temperature was accurately predicted by the developed ANN model, with the predictions closely aligning with the experimental values. Although the experimental dataset includes only a limited number of data points for these conditions, the ANN model successfully predicted creep life for 100 different data points within the same temperature range. The high accuracy of the model's predictions is evident from the results shown in Figure 5, where the predicted values align closely with the expected trends. Similarly, the ANN model can provide accurate predictions for different applied stress levels to estimate the creep rupture life of 5Cr-0.5Mo steel. This enables the assessment of the remaining creep life of components made from this steel at specific temperatures and under any given applied stress condition.

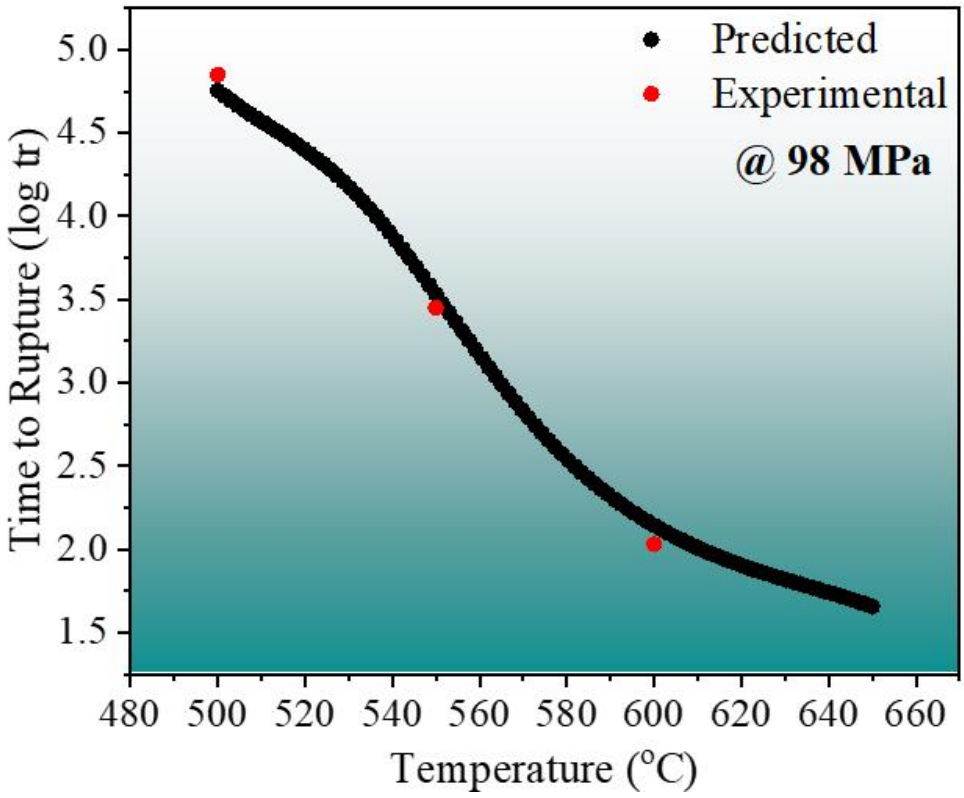

Figure 5. Graphical representation of the effect of temperature on the creep rupture life under a stress of 98 MPa. The red color is for experimental and the black color is for prediction from ANN model.

Moreover, the impact of the most critical alloying elements, C and Si, on creep rupture life can also be accurately predicted using the ANN model. C forms various metal carbides, such as $M_{23}C_6$, which precipitate and disperse within the matrix [30]. These carbides effectively hinder dislocation motion and restrict the movement of lath boundaries [31, 32], thereby enhancing the material's resistance to deformation and ultimately increasing the creep rupture life. Additionally, coarse carbides can contribute to strengthening through Ostwald ripening, which further improves the creep rupture life of the steel [33]. Si also significantly influences the creep rupture life under fixed temperature and stress conditions. The positive effect of Si arises from its ability to lower the stacking fault energy, which promotes the formation of deformation twins [34]. These stacking faults and twins act as barriers to dislocation motion, thereby delaying the rupture of the steel and enhancing its creep resistance. A similar beneficial effect of Si on creep rupture life at 550°C has been reported in previous studies [35]. Figure 6 illustrates the precise predictions of the model regarding the effect of C content (Fig.6a) and Si content (Fig.6b) on creep rupture life at 550 ºC and under a fixed stress of 98 MPa. This predictive capability allows users to estimate the creep rupture life of steel with a known C content or to evaluate how C content influences creep life at a specific temperature or applied stress. Such insights are particularly useful for optimizing alloy compositions for desired performance under varying service conditions.

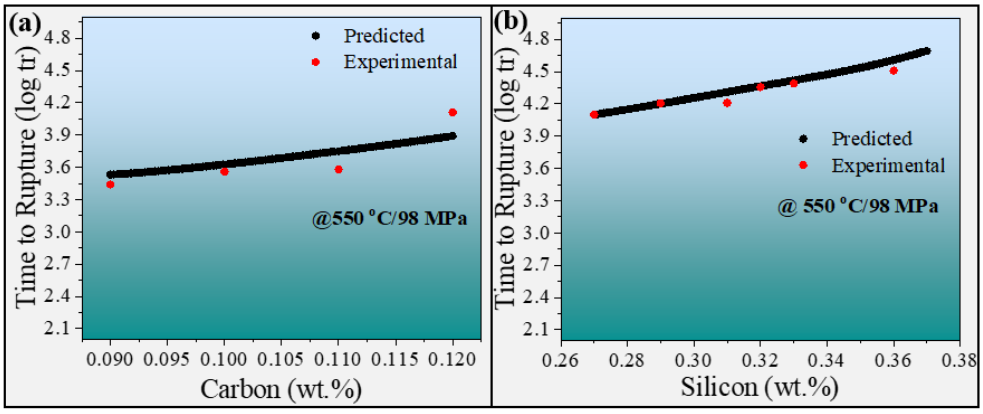

Figure 6. Graphical representation of the effect of carbon content on the creep rupture life at 550 ºC and under a stress of 98 MPa. The red color is for experimental and the black color is for prediction from ANN model.

4.3. Prediction of the combined effect of two variables on Creep Rupture life

The combined effect of two input variables, such as temperature and stress, is often complex and challenging to predict due to their intricate interdependencies. However, the developed ANN model successfully predicted this combined effect with remarkable accuracy, as demonstrated by the contour plots in Figure 7. These plots clearly illustrate the model's capability to capture and represent the interplay between temperature and applied stress in determining the creep rupture life, further validating its predictive robustness and utility in practical applications.

The inverse relationship between stress and temperature on creep rupture life is clearly depicted in the single-variable graphs (Fig. 4 and Fig. 5). Additionally, the combined inverse effect of both temperature and stress is illustrated in the contour plot (Figure 7(a)), where the highest creep rupture life values are observed at lower stress levels (50–100 MPa) and lower temperatures (500–550 °C). This trend aligns well with the literature, as at higher values of both stress and temperature, dislocation motion becomes easier and faster, leading to earlier rupture and a subsequent decrease in creep rupture life.

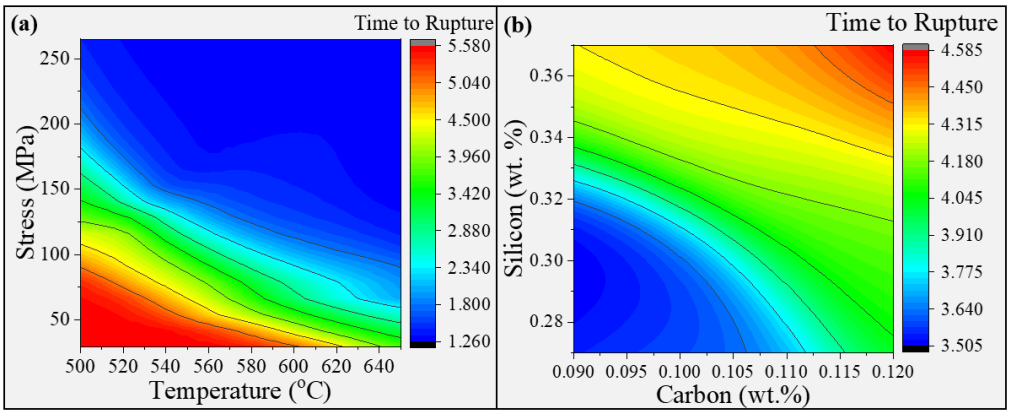

Figure 7. Contour plots showing the combined effect of (a) temperature and stress, (b) carbon and silicon content, on the creep rupture life of 5Cr-0.5Mo steel.

Similarly, the combined effect of C and Si content on the creep rupture life is also accurately predicted. The contour plot in Figure 7(b) illustrates those higher levels of C and Si result in longer rupture times for 5Cr-0.5Mo steel. This prediction is consistent with the literature [36, 37], as Si and C contribute to the formation of precipitates/carbides that hinder dislocation motion, thereby delaying fracture and enhancing creep

strength. In addition, the combined effects of other input parameters can also be predicted. However, to maintain conciseness, the corresponding graphs are not included in the manuscript. To illustrate the combined effect of carbon and phosphorus, a contour plot is provided as a supplementary Figure 1, demonstrating that an increased phosphorus content enhances creep rupture life due to the formation of precipitates. Likewise, the interactions between all minor alloying elements can be precisely estimated for nearly 100 different scenarios, a level of detail that is not achievable through experimental methods. This underscores the reliability and effectiveness of the developed ANN model.

4.4. Quantitative estimation of the effect of temperature and stress

The quantitative effects of both temperature and stress were also evaluated using the ANN model, as presented in Tables 2 and 3. The temperature was incremented in intervals of 50 °C, ranging from 500 °C to 650 °C, and the relative percentage error for the predictions was calculated to be very low at 3.64%. Similarly, Table 3 highlights the quantitative effect of stress on the creep rupture life of 5Cr-0.5Mo steel, with stress values increased in varying intervals. The relative percentage error for stress predictions was just 1.78%, demonstrating the high accuracy and reliability of the developed ANN model. The percentage relative error was calculated by using the formula given in Equation 6.

$$Percentage\ Relative\ Error = \frac{Actual\ Value - Predicted\ Value}{Actual\ Value} \times 100 \quad (6)$$

Table 2. Effect of temperature on the Creep Rupture life under 29 MPa stress.

Stress	Time to Rupture	Difference
5Cr-0.5Mo steel at 500 ºC	5.576	-
5Cr-0.5Mo steel at 550 ºC	5.567	-0.009
5Cr-0.5Mo steel at 600 ºC	5.024	-0.543
5Cr-0.5Mo steel at 650 ºC	3.709	-1.315
Experimental time to rupture	3.849	
Absolute Error in prediction	3.849-3.709 = 0.14	
Percentage Relative Error	0.14/3.849*100=**3.64%**	

Table 3. Effect of applied stress on the Creep Rupture life at 500 ºC

Stress	Time to Rupture	Difference
5Cr-0.5Mo steel under 30 MPa	5.576	-
5Cr-0.5Mo steel under 50 MPa	5.575	-0.001
5Cr-0.5Mo steel under 100 MPa	4.656	-0.919
5Cr-0.5Mo steel under 130 MPa	3.789	-0.867
5Cr-0.5Mo steel under 150 MPa	3.204	-0.585
5Cr-0.5Mo steel under 200 MPa	1.913	-1.291
5Cr-0.5Mo steel under 216 MPa	1.706	-0.207
Experimental Value under 216 MPa	1.737	
Absolute Error in Prediction	1.737 – 1.706 = 0.031	
Percentage Relative Error	0.031/1.737*100 = **1.78%**	

4.5. Graphical User Interface

Figure 8 presents the graphical user interface (GUI) of the developed ANN model, designed to predict creep rupture life based on 16 input variables. The GUI enables users to input infinite parameter combinations for precise predictions and dynamically

visualize output variations as inputs are modified. It allows for analyzing the impact of individual variables by varying one while keeping others constant and evaluating the combined effect of two variables to gain deeper insights. Additionally, users can optimize specific parameters to achieve target creep rupture life, assess the relative importance of each variable, and compare predictions across multiple input configurations for a comprehensive evaluation of material compositions and operating conditions.

The GUI is highly user-friendly and intuitive, requiring no prior knowledge of machine learning, which makes it ideal for industrial applications. The model predicts the creep rupture life in terms of the logarithm of time to rupture—a critical parameter for materials scientists to evaluate, optimize, and select material compositions. This capability supports material design, process optimization, and failure prevention in high-temperature applications.

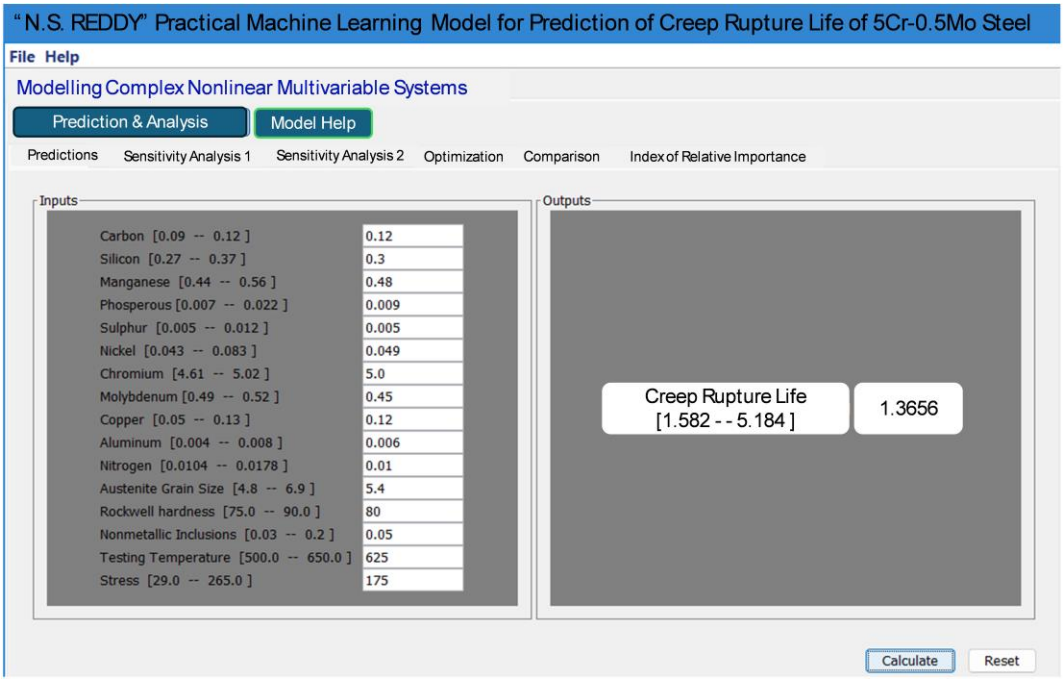

Figure 8. Screenshot of the graphical user interface (GUI) of the developed model.

4.5. Optimization of inputs to get maximum creep rupture life

The developed GUI can optimize input parameters for superior performance. The highest experimental creep rupture life in the dataset was 152,683 hours. However, using the optimization module within the GUI, the model predicted a significantly higher creep rupture life of 410,865 hours (log 5.6137 as shown in Figure 9), showcasing the potential of ANN-driven optimization in identifying material configurations beyond the experimental limits.

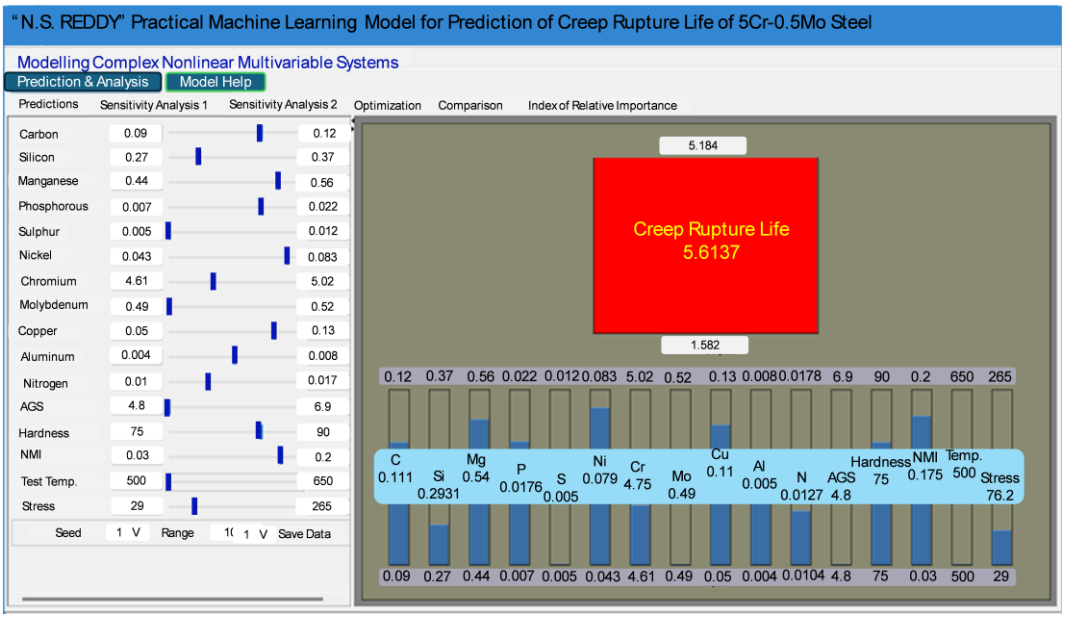

Figure 9. Screenshot of the optimized inputs for the maximum creep rupture life.

The optimization process systematically adjusted the 16 input parameters—material compositions (e.g., C, Si, Mn, S, Ni, etc.), operating conditions (e.g., stress and testing temperature), and material properties (e.g., Rockwell hardness, AGS)—to find the most favorable combination for extended creep rupture life. This capability highlights the ANN model's proficiency in capturing complex nonlinear interactions among multiple variables. The ability to achieve a creep rupture life significantly higher than the experimental maximum underscores the utility of this tool for advanced material research and engineering applications.

5. Conclusions

In conclusion, this study employed six different machine learning models—Gradient Boosting (GB), Random Forest (RF), Linear Regression (LR), Extreme Gradient Boosting (XGB), AdaBoost (AB), and Artificial Neural Network (ANN)—to predict the creep rupture life of 5Cr-0.5Mo steel. Among these, the ANN model demonstrated the highest efficiency, achieving minimal prediction errors for the test dataset (RMSE = 0.069, MAE = 0.053, MAPE = 0.014, and R^2 = 1. The developed ANN model effectively predicted the influence of composition, including minor alloying elements such as carbon and silicon, as well as the effects of temperature and applied stress. It accurately captured both the impact of individual input variables and the combined effects of two variables, such as temperature and stress, or alloying elements like carbon and phosphorus. Additionally, a user-friendly graphical user interface (GUI) was developed, enabling engineers and industry professionals to optimize alloy composition based on the desired creep rupture life of 5Cr-0.5Mo steel.

Supplementary Materials: The supporting information can be downloaded at: www.mdpi.com/xxx/s1, Appendix A1. Data used for Model development and testing. Figure S1. Contour plot showing the combined effect of carbon and Phosphorous content on the creep rupture life of 5Cr-0.5Mo steel.

Author Contributions: Conceptualization, M.I. and N.S.R.; methodology, M.I. and H.M.R.T.; software, N.S.R.; validation, H.M.R.T.; formal analysis, M.I. and D.Y.C. R; investigation, M.I. and D.Y.C. R.; resources, S.G.K.; data curation, M.I. and H.M.R.T.; writing—original draft preparation, M.I..;

writing—review and editing, S.G.K. and N.S.R.; supervision, N.S.R. and S.G.K. All authors have read and agreed to the published version of the manuscript.

Funding: This research received no external funding.

Data Availability Statement: The original contributions presented in this study are included in the article. Further inquiries can be directed to the corresponding author.

Conflicts of Interest: The authors declare no conflicts of interest.

Abbreviations

The following abbreviations are used in this manuscript:

ANN	Artificial Neural Network
LR	Linear Regression
AB	Ada Boost
RF	Random Forest
GB	Gradient boosting
NIMS	National Institute for Materials Science
NMI	Nonmetallic Inclusions
AGS	Austenite Grain Size
HRB	Hardness Rockwell Scale B
RMSE	Root Mean Square Error
adj. R^2	Adjusted R-squared

References

1. HKDH, B., Design of ferritic creep-resistant steels. *ISIJ international* **2001,** 41, (6), 626-640.
2. Masuyama, F., History of power plants and progress in heat resistant steels. *ISIJ international* **2001,** 41, (6), 612-625.
3. Xia, T.; Ma, Y.; Zhang, Y.; Li, J.; Xu, H., Effect of Mo and Cr on the Microstructure and Properties of Low-Alloy Wear-Resistant Steels. *Materials* **2024,** 17, (10), 2408.
4. Ishtiaq, M.; Inam, A.; Tiwari, S.; Seol, J. B., Microstructural, mechanical, and electrochemical analysis of carbon doped AISI carbon steels. *Applied Microscopy* **2022,** 52, (1), 10.
5. Wang, H.; Cao, L.; Li, Y.; Schneider, M.; Detemple, E.; Eggeler, G., Effect of cooling rate on the microstructure and mechanical properties of a low-carbon low-alloyed steel. *Journal of Materials Science* **2021,** 56, (18), 11098-11113.
6. Yamabe, J.; Matsunaga, H.; Furuya, Y.; Hamada, S.; Itoga, H.; Yoshikawa, M.; Takeuchi, E.; Matsuoka, S., Qualification of chromium–molybdenum steel based on the safety factor multiplier method in CHMC1-2014. *International Journal of Hydrogen Energy* **2015,** 40, (1), 719-728.
7. Matsunaga, H.; Yoshikawa, M.; Kondo, R.; Yamabe, J.; Matsuoka, S., Slow strain rate tensile and fatigue properties of Cr–Mo and carbon steels in a 115 MPa hydrogen gas atmosphere. *International Journal of Hydrogen Energy* **2015,** 40, (16), 5739-5748.
8. Xia, Z.-X.; Wang, C.-Y.; Zhao, Y.-F.; Zhang, G.-D.; Zhang, L.; Meng, X.-M., Laves Phase Formation and Its Effect on Mechanical Properties in P91 Steel. *Acta Metallurgica Sinica (English Letters)* **2015,** 28, (10), 1238-1246.
9. Tanaka, K.; Shimonishi, D.; Nakagawa, D.; Ijiri, M.; Yoshimura, T., Stress Relaxation Behavior of Cavitation-Processed Cr–Mo Steel and Ni–Cr–Mo Steel. *Applied Sciences* **2019,** 9, (2), 299.
10. Jacob, K.; Roy, A.; Gururajan, M. P.; Jaya, B. N., Effect of dislocation network on precipitate morphology and deformation behaviour in maraging steels: Modelling and experimental validation. *Materialia* **2022,** 21, 101358.
11. Saucedo-Muñoz, M. L.; Lopez-Hirata, V. M.; Dorantes-Rosales, H. J.; Villegas-Cardenas, J. D.; Rivas-Lopez, D. I.; Beltran-Zuñiga, M.; Ferreira-Palma, C.; Moreno-Palmerin, J., Phase Transformations of 5Cr-0.5Mo-0.1C Steel after Heat Treatment and Isothermal Exposure. *Metals* **2022,** 12, (8), 1378.

12. Ishtiaq, M.; Kim, Y.-K.; Tiwari, S.; Lee, C. H.; Jo, W. H.; Sung, H.; Cho, K.-S.; Kang, S.-G.; Na, Y.-S.; Seol, J. B., Serration-induced plasticity in phase transformative stainless steel 316L upon ultracold deformation at 4.2 K. *Materials Science and Engineering: A* **2025,** 921, 147591.
13. Baltušnikas, A.; Grybėnas, A.; Kriūkienė, R.; Lukošiūtė, I.; Makarevičius, V., Evolution of Crystallographic Structure of M23C6 Carbide Under Thermal Aging of P91 Steel. *Journal of Materials Engineering and Performance* **2019,** 28, (3), 1480-1490.
14. Thomson, R. C.; Miller, M. K., Carbide precipitation in martensite during the early stages of tempering Cr- andMo-containing low alloy steels. *Acta Materialia* **1998,** 46, (6), 2203-2213.
15. Abe, F., Coarsening behavior of lath and its effect on creep rates in tempered martensitic 9Cr–W steels. *Materials Science and Engineering: A* **2004,** 387-389, 565-569.
16. Parker, J., In-service behavior of creep strength enhanced ferritic steels Grade 91 and Grade 92 – Part 1 parent metal. *International Journal of Pressure Vessels and Piping* **2013,** 101, 30-36.
17. Das, S. K.; Joarder, A.; Mitra, A., Magnetic Barkhausen emissions and microstructural degradation study in 1.25 Cr–0.50 Mo steel during high temperature exposure. *NDT & E International* **2004,** 37, (3), 243-248.
18. Viswanathan, R., Effect of stress and temperature on the creep and rupture behavior of a 1.25 Pct chromium—0.5 Pct molybdenum steel. *Metallurgical Transactions A* **1977,** 8, (6), 877-884.
19. Mohapatra, J. N.; Panda, A. K.; Gunjan, M. K.; Bandyopadhyay, N. R.; Mitra, A.; Ghosh, R. N., Ageing behavior study of 5Cr–0.5Mo steel by magnetic Barkhausen emissions and magnetic hysteresis loop techniques. *NDT & E International* **2007,** 40, (2), 173-178.
20. Das, G.; Rao, V.; Joarder, A.; Mohanty, O. N.; Murthy, S. G. N.; Mitra, A., Magnetic characterization of 5Cr-0.5Mo steel used in process heater tubes. *Journal of Physics D: Applied Physics* **1995,** 28, (11), 2229.
21. Hamzah, M. Z.; Yeo, W. H.; Fry, A. T.; Inayat-Hussain, J. I.; Ramesh, S.; Purbolaksono, J., Estimation of oxide scale growth and temperature increase of high (9–12%) chromium martensitic steels of superheater tubes. *Engineering Failure Analysis* **2013,** 35, 380-386.
22. Ishtiaq, M.; Tiwari, S.; Panigrahi, B. B.; Seol, J. B.; Reddy, N. S., Neural Network-Based Modeling of the Interplay between Composition, Service Temperature, and Thermal Conductivity in Steels for Engineering Applications. *International Journal of Thermophysics* **2024,** 45, (10), 137.
23. Guo, S.; Yu, J.; Liu, X.; Wang, C.; Jiang, Q., A predicting model for properties of steel using the industrial big data based on machine learning. *Computational Materials Science* **2019,** 160, 95-104.
24. Wang, S.; Li, J.; Zuo, X.; Chen, N.; Rong, Y., An optimized machine-learning model for mechanical properties prediction and domain knowledge clarification in quenched and tempered steels. *Journal of Materials Research and Technology* **2023,** 24, 3352-3362.
25. Gao, X.-y.; Fan, W.-b.; Xing, L.; Tan, H.-j.; Yuan, X.-m.; Wang, H.-y., Construction of a prediction model for properties of wear-resistant steel using industrial data based on machine learning approach. *Journal of Iron and Steel Research International* **2024**.
26. Zhang, X.-C.; Gong, J.-G.; Xuan, F.-Z., A deep learning based life prediction method for components under creep, fatigue and creep-fatigue conditions. *International Journal of Fatigue* **2021,** 148, 106236.
27. Tan, Y.; Wang, X.; Kang, Z.; Ye, F.; Chen, Y.; Zhou, D.; Zhang, X.; Gong, J., Creep lifetime prediction of 9% Cr martensitic heat-resistant steel based on ensemble learning method. *Journal of Materials Research and Technology* **2022,** 21, 4745-4760.
28. Xiang, S.; Chen, X.; Fan, Z.; Chen, T.; Lian, X., A deep learning-aided prediction approach for creep rupture time of Fe–Cr–Ni heat-resistant alloys by integrating textual and visual features. *Journal of Materials Research and Technology* **2022,** 18, 268-281.
29. Wang, C.; Wei, X.; Ren, D.; Wang, X.; Xu, W., High-throughput map design of creep life in low-alloy steels by integrating machine learning with a genetic algorithm. *Materials & Design* **2022,** 213, 110326.
30. Zhao, L.; Wei, S.; Gao, D.; Lu, S., Effect of Carbon Content on the Creep Rupture Properties and Microstructure of 316H Weld Metals. *Acta Metallurgica Sinica (English Letters)* **2021,** 34, (7), 986-996.

31. Mitsuhara, M.; Yamasaki, S.; Miake, M.; Nakashima, H.; Nishida, M.; Kusumoto, J.; Kanaya, A., Creep strengthening by lath boundaries in 9Cr ferritic heat-resistant steel. *Philosophical Magazine Letters* **2016,** 96, (2), 76-83.
32. Dudko, V.; Belyakov, A.; Kaibyshev, R., Evolution of Lath Substructure and Internal Stresses in a 9% Cr Steel during Creep. *ISIJ International* **2017,** 57, (3), 540-549.
33. Semba, H.; Abe, F., Alloy design and creep strength of advanced 9%Cr USC boiler steels containing high concentration of boron. *Energy Materials* **2006,** 1, (4), 238-244.
34. Kalandyk, B.; Zapała, R.; Starowicz, M., The Effect of Si and Mn on Microstructure and Selected Properties of Cr-Ni Stainless Steels. *Archives of Foundry Engineering* **2017,** 17.
35. Lu, C.; Yi, H.; Chen, M.; Xu, Y.; Wang, M.; Hao, X.; Liang, T.; Ma, Y., Effects of Si on the stress rupture life and microstructure of a novel austenitic stainless steel. *Journal of Materials Research and Technology* **2023,** 25, 3408-3424.
36. Pilling, J.; Ridley, N.; Gooch, D. J., The effect of phosphorus on creep in 2.25%Cr-1% Mo steels. *Acta Metallurgica* **1982,** 30, (8), 1587-1595.
37. Latha, S.; Nandagopal, M.; Parameswaran, P.; Reddy, G. V. P., Effect of P and Si on creep induced precipitation in 20% CW Ti-modified 14Cr-15Ni stainless steel fast reactor clad. *Materials Science and Engineering: A* **2019,** 759, 736-744.